Cytidine-Directed Rapid Synthesis of Water-Soluble and Highly Yellow Fluorescent Bimetallic AuAg Nanoclusters

ARTICLE *in* LANGMUIR · AUGUST 2014

Impact Factor: 4.46 · DOI: 10.1021/la5028702 · Source: PubMed

Langmuir

Article

pubs.acs.org/Langmuir

Cytidine-Directed Rapid Synthesis of Water-Soluble and Highly Yellow Fluorescent Bimetallic AuAg Nanoclusters

Yuanyuan Zhang, Hui Jiang, Wei Ge, Qiwei Li, and Xuemei Wang*

State Key Lab of Bioelectronics (Chien-Shiung Wu Laboratory), Southeast University, No. 2 Sipailou, Nanjing 210096, P. R. China

Supporting Information

ABSTRACT: Fluorescent gold/silver nanoclusters templated by DNA or oligonucleotides have been widely reported since DNA or oligonucleotides could be designed to position a few metal ions at close proximity prior to their reduction, but nucleoside-templated synthesis is more challenging. In this work, a novel type of strategy taking cytidine (C) as template to rapid synthesis of fluorescent, water-soluble gold and silver nanoclusters (C-AuAg NCs) has been developed. The as-prepared C-AuAg NCs have been characterized by UV−vis absorption spectroscopy, fluorescence, transmission electron microscopy (TEM), energy dispersive X-ray spectroscopy (EDS), X-ray photoelectron spectroscopy (XPS), Fourier transform infrared spectroscopy (FT-IR), and inductively coupled plasma mass spectroscopy (ICP-MS). The characterizations demonstrate that C-AuAg NCs with a diameter of 1.50 ± 0.31 nm, a quantum yield ∼9%, and an average lifetime ∼6.07 μs possess prominent fluorescence properties, good dispersibility, and easy water solubility, indicating the promising application in bioanalysis and biomedical diagnosis. Furthermore, this strategy by rapid producing of highly fluorescent nanoclusters could be explored for the possible recognition of some disease-related changes in blood serum. This raises the possibility of their promising application in bioanalysis and biomedical diagnosis.

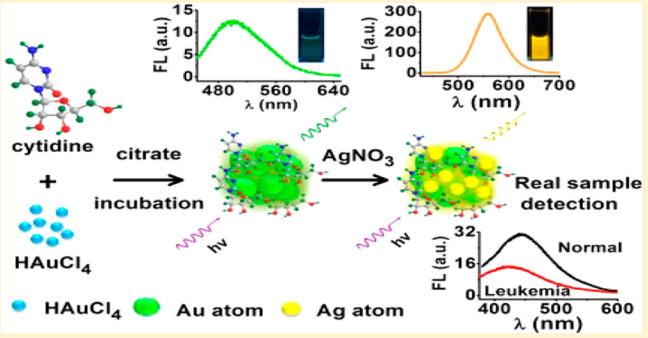

INTRODUCTION

Metal nanoclusters (NCs) have attracted much interest because they provide the missing link between atomic and nanoparticle behavior in metals.[1−3] Composed of a few to a hundred atoms, their dimensions approach the Fermi wavelength of electrons, resulting in molecule-like properties such as discrete electronic states and size-dependent fluorescence that is dramatically different from nanoparticles with diameters greater than 2 nm.[4,5] Fluorescent metal NCs have a set of fascinating features, such as ultrasmall size, good biocompatibility, and excellent photostability, making them attracted intense interest in areas such as molecular recognition,[6−8] metal ions detection,[9−11] bioimaging,[12,13] and catalysis.[14−16] Among various metallic NCs, Au and Ag NCs are the most popular, mainly because of their strong fluorescence properties, stability, and biocompatibility. Researchers have developed various approaches to synthesize water-soluble fluorescent metal NCs.[4,17] Template-based synthetic strategies have led to the preparation of fluorescent, water-soluble Au or Ag NCs.[1−3,5] In general, the reduction of metal ions in aqueous solution results in large nanoparticles rather than small NCs due to the tendency of NCs to aggregate.[1] In addition, the nature of the ligands used for capping the particle surface can markedly affect their emission properties.[18] Therefore, choosing suitable agents capable of stabilizing clusters from aggregating and enhancing their fluorescence is of key importance for obtaining small, highly fluorescent metal NCs.[1] The various synthetic strategies for fluorescent metal NCs, such as Au NCs or Ag NCs, based on different types of stabilizers was discussed. The mainly stabilizers have been reported at present including the most commonly adopted stabilizers thiol-containing small molecules owing to the strong interaction between thiols and Au/Ag,[11,17,19] dendrimers based on their capability of sequestering metal ions from solution,[20] polymers with abundant carboxylic acid groups,[21] biological macromolecules such as peptides and proteins,[6,7,22,23] and DNA due to the well-known interactions with metal cations.[24−26]

DNA-templated fluorescent Au and Ag NCs with good biocompatibility, stable against aggregation, large Stokes shift, and high emission rates have been widely studied.[1,4,24,25] Researches have indicated that metal ions possess a high affinity to cytosine bases on single-stranded DNA, which makes DNA oligonucleotides good stabilizers for preparing small metal NCs.[25−27] Gwinn and co-workers[28,29] reported single-strand RNAs host fluorescent silver nanoclusters, analogous to previously studied Ag:DNAs, and further they used tandem HPLC−mass spectrometry with in-line spectroscopy to identify silver atom numbers of 10−21 in visible- to infrared-emitting Ag:DNA complexes stabilized by oligonucleotide monomers and dimers. Liu and co-workers[26] showed that blue fluorescent

Received: April 24, 2014
Revised: August 23, 2014
Published: August 26, 2014

   dx.doi.org/10.1021/la5028702 | Langmuir 2014, 30, 10910−10917

Scheme 1. Schematic of the Synthesis of Fluorescent C-AuAg NCs

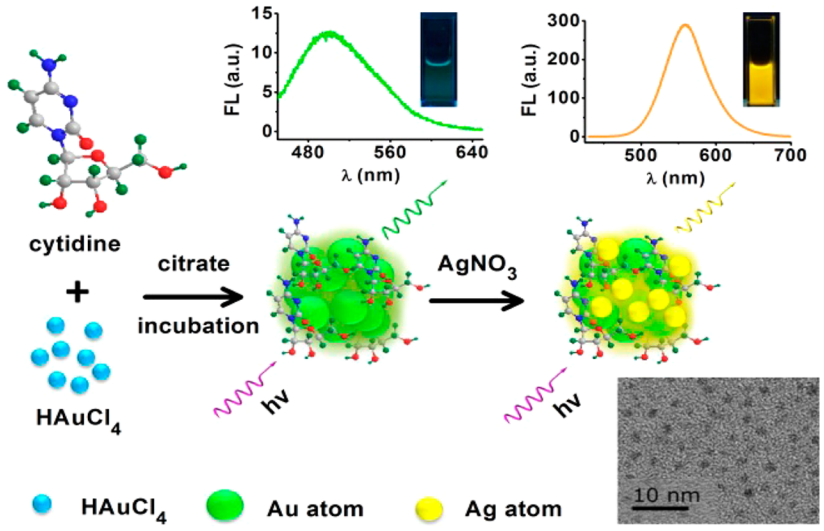

gold nanoclusters could be prepared in the presence of polycytosine DNAs at low pH using citrate as the reducing agent. In addition, several studies were carried out that emphasize the key role of bases and base sequences on the formation of oligonucleotide-stabilized fluorescent Ag NCs.[30−32] For instance, Petty and co-workers[32] found the dominant influence of bases on Ag cluster formation. Although fluorescent gold/silver nanoclusters templated by DNA have been widely reported,[4,24−29] nucleotide-templated synthesis is more challenging since DNA could be designed to position a few metal ions at close proximity prior to their reduction. For nucleotides, gold/silver needs to be made close to each other by multivalent coordination. Liu and co-workers[33] have reported the synthesis of Au NCs with average size of 2 nm template by ATP under citrate reduce and light exposure. But there is no report about gold/silver NCs template by nucleoside, in addition of above reports focusing on fluorescence gold or silver nanoclusters template by DNA, oligonucleotides, or nucleotide.

Nucleoside (e.g., adenosine, cytidine, uridine, or guanosine) is the primary unit of RNA, which will be released through the degradation of tRNA and eliminated from the body with human urine. It is notable that the concentration of modified nucleoside will apparently increase when human body turns up cancerization promoting the degradation of tRNA.[34,35] Therefore, the relevant changes reflect the physical health condition to some extent.

On the basis of the above consideration, in this study we put forward the most characterized experimental investigation of the rapidly producing bimetallic AuAg nanoclusters with high fluorescence through template by cytidine (C-AuAg NCs). The as-prepared C-AuAg NCs have a diameter of 1.50 ± 0.31 nm, a quantum yield ∼9%, and an average lifetime ∼6.07 μs with prominent fluorescence properties, good dispersibility, and easy water solubility. Special attention was paid to the optical and structural properties of these clusters. Compared with the luminescent AuAg NCs reported,[10,13,36] our green synthesis strategy is rapid (ca. 1 h) and easy operation. The availability of both nanoclusters and molecular species allows us to employ a diverse range of techniques to gain a more complete understanding of relevant bioprocess. Our observations demonstrate that this strategy by rapid producing of highly fluorescent nanoclusters could be further explored for the possible recognition of some disease related changes in blood serum, indicating the potential and promising application in relevant bioanalysis and biomedical diagnosis.

EXPERIMENTAL SECTION

Chemicals and Materials. All ribonucleosides (adenosine, cytidine, uridine, guanosine, or thymidine) were purchased from Sigma-Aldrich and were used as received. Auric chloride acid ($HAuCl_4 \cdot 6H_2O$) and silver nitrate ($AgNO_3$), trisodium citrate, citric acid, and ethylenediaminetetraacetic acid (EDTA) were purchased from Sinopharm Chemical Reagent Co., Ltd. Phosphate buffer solution (PBS) (pH 7.4, 0.02 M) comprising NaH_2PO_4 and Na_2HPO_4 was used as the supporting electrolyte. All the solutions were prepared by doubly distilled water.

Synthesis of C-AuAg NCs. The synthesis of C-AuAg NCs is as follows. First, 40 μL of 50 mM cytidine was added in 1.56 mL of water or PBS (final concentration: 1 mM). To this mixture, 100 μL of 5 mM $HAuCl_4$ was added (final concentration: 0.25 mM) followed by 200 μL of 0.5 M citrate buffer (pH 6, final concentration: 50 mM, pH 6.5). Then heat the mixture under 80 °C water bath for a certain time followed by addition of 100 μL of 5 mM $AgNO_3$ (final concentration: 0.25 mM) after heating to make up a final volume of 2.0 mL. The cytidine-mediated luminescent AuAg nanoclusters were formed.

Several parameters (e.g., cytidine, $HAuCl_4$, and $AgNO_3$ concentration) were varied before the optimized values above were obtained. For other nucleosides (adenosine, uridine, guanosine, or thymidine), the procedure was similar.

Filtration To Remove Large Aggregates, Free Cytidine, and Excess Citrate. The solution was filtered by a 0.22 μm filter and further centrifuged by an ultrafilter (Pall Corporation, formula weight cutoff 10 kDa) to cut down the insoluble aggregates. It is noted that the insoluble aggregate is the precipitate of AgCl formed upon addition of $AgNO_3$ to the C-Au NCs solution, and the relative amount of insoluble aggregates is about 2.7% to the $HAuCl_4$. To avoid the interference from the free cytidine and citrate, the supernatant was further purified by adding an amount of ethanol into the aqueous solution (the ratio between water and ethanol is 1:1) and centrifuged at 8000 rpm for 10 min. Under such condition, the cytidine-mediated fluorescent AuAg nanoclusters were precipitated out of the solution while the free cytidine and excessive citrate remained in the solution. The precipitates were then resuspended in aqueous solution to obtain the final solution contained cytidine-mediated luminescent AuAg nanoclusters (C-AuAg NCs).

Real Sample Detection. Fresh serum samples of 40 μL were added in 1.56 mL of PBS. To this mixture, 100 μL of 5 mM $HAuCl_4$

dx.doi.org/10.1021/la5028702 | Langmuir 2014, 30, 10910−10917

was added, followed by 200 μL of 0.5 M citrate buffer (pH 6). Then the mixture was incubated under 37 °C water bath for 1 h followed by 100 μL of 5 mM $AgNO_3$ being added as soon as incubation was stopped to make up a final volume of 2.0 mL. Finally, the samples were measured by a fluorometer.

Characterization. Fluorescence measurements were carried out using Shimadzu RF-5301 PC instrument. The slit wavelength for excitation and emission was set as 3 nm. Fourier transform infrared spectroscopy (FT-IR) spectra were measured using a KBr pellet with a Nicolet 5700 instrument. A Thermo BioMate 3S UV−vis spectrophotometer was used for the UV−vis adsorption measurements. Spectra were typically measured in the range of 200−600 nm. Transmission electron microscopy (TEM) images were collected using a JEM-2100 microscope to characterize the size and size distribution. A diluted solution was spotted on carbon-coated copper grid (300 mesh) and was dried in laboratory ambience. Energy dispersive X-ray spectroscopy (EDS) analyses were done in a Zeiss Ultra Plus scanning electron microscope (SEM). For measurements, samples were drop-casted on a silicon wafer and dried in laboratory ambience. The X-ray photoelectron spectroscopic data are recorded on a PHI 5000 Versa Probe X-ray photoelectron spectrometer (XPS) with an Al Kα = 280.00 eV excitation source. Binding energies of the core levels were calibrated with C 1s binding energy (BE) set at 284.0 eV. For measurements, the sample was prepared by coating a layer of C-AuAg NCs on silicon wafer and dried in laboratory ambience. The quantum yield (QY) of fluorescent C-AuAg NCs prepared in a typical procedure was measured using Rhodamine B as a reference standard (QY: 95% in ethanol). Fluorescence lifetimes were recorded at room temperature using an FLS920 fluorescence spectrometer (Edinburgh Instruments Ltd., United Kingdom), with excitation at 370 nm and detection at the C-AuAg NCs maxima. The data were fitted with a single-exponential decay, and χ^2 was less than 1.2. The composition of the NCs was analyzed by inductively coupled plasma mass spectroscopy (ICP -MS) on an Optima 5300DV.

RESULTS AND DISCUSSION

The bimetallic C-AuAg NCs, which are reduced by citrate and template by cytidine, exhibit stable and bright fluorescence. The synthesis procedure of C-AuAg NCs is described in Scheme 1, where the initial step is the synthesis of Au nanoclusters, taken cytidine as a template and reduced by citrate, and then followed by heating at 80 °C in water bath for a certain time to form C-Au nanoclusters solution. Afterward, adding an equivalent amount of $AgNO_3$ to the as-synthesized solution, surprisingly the stable ultrasmall fluorescent C-AuAg nanoclusters could be readily and rapidly obtained (for details see the Experimental Section).

Interestingly, it is observed that among the template of adenosine (A), cytidine (C), uridine (U), guanosine (G), or thymidine (T), only cytidine and adenosine as template can produce AuAg fluorescent products with yellow and green fluorescence, respectively. Under the UV lamp, a bright yellow and green fluorescence from the as-prepared nucleoside−AuAg solutions could be readily observed by the naked eye (Figure 1, inset), indicating a highly luminescent species formed. In contrast, uridine, guanosine, and thymidine fail to produce fluorescence products (Figure S1A, Supporting Information). The fluorescence spectrum of the C-AuAg NCs shows an emission and excitation maxima wavelength at 560 and 370 nm, respectively (Figure 1, black trace). A-AuAg solution shows an emission and excitation maxima wavelength at 480 and 350 nm, respectively (Figure 1, red trace).

Meanwhile, it is noted that there exists an apparent different effect upon the sequence of adding $HAuCl_4$ and $AgNO_3$ when cytidine and adenosine are taken as templates for the relevant solution. The optical and fluorescence photographs of C-Au, C-Ag, A-Au, and A-Ag products reduced with pH 6 citrate buffer for 1 h incubation at 80 °C are demonstrated in Figure 2A,

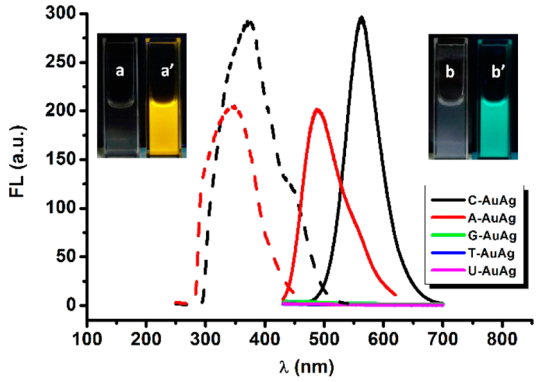

Figure 1. Fluorescence emission (solid line) and excitation (dotted line) spectra of ribonucleoside−AuAg solution. Only cytidine (black trace) and adenosine (red trace) produce fluorescence. Inset: fluorescence (excited at 365 nm; a′, b′) and optical (a, b) photographs of the solution of C-AuAg (a, a′) and A-AuAg (b, b′).

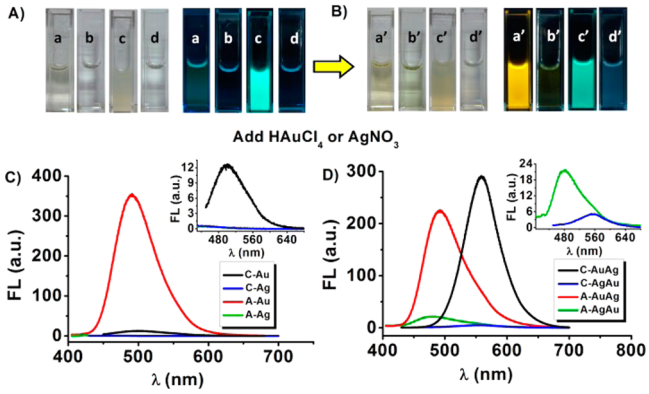

Figure 2. Optical (A, left, and B, left) and fluorescence (excited at 365 nm; A, right, and B, right) photographs of (A) C-Au (a), C-Ag (b), A-Au (c), A-Ag (d) solution reduced with pH 6 citrate buffer after 1 h incubation at 80 °C water bath and (B) that of C-AuAg (a′), C-AgAu (b′), A-AuAg (c′), A-AgAu (d′) solution upon addition of $HAuCl_4$ or $AgNO_3$ to the corresponding solution in (A). (C) and (D) are the relevant fluorescence emission spectra of C-Au, C-Ag, A-Au, A-Ag and C-AuAg, C-AgAu, A-AuAg, A-AgAu. Inset in (C) and (D) is the enlarged view of C-Au, C-Ag, A-Ag and C-AgAu, A-AgAu, respectively. The concentration of both cytidine and adenosine is 1 mM, while the concentration of $HAuCl_4$ and $AgNO_3$ is 0.25 mM and that of citrate buffer is 50 mM.

while that of C-AuAg, C-AgAu, A-AuAg, and A-AgAu is illustrated in Figure 2B. An amazing discovery is that initially C-Au solution has very weak fluorescence (inset in Figure 2C, black trace) which is almost invisible by the naked eye under a UV lamp (Figure 2A-a), but an intense yellow fluorescence emerges immediately upon addition of $AgNO_3$ (Figure 2B-a′), with the maximum fluorescence amplitudes increase for about 25-fold (Figure 2D, black trace). Importantly, the solution is transparent and the excitation of C-AuAg NCs at different wavelengths does not affect the peak wavelength of the emission spectrum (Figure S2, Supporting Information), indicating the relatively high stability of these C-AuAg metal nanoclusters. Moreover, upon addition of $HAuCl_4$ to cytidine solution, the absorption peak of cytidine red-shift from 271 to 278 nm, and the addition of $AgNO_3$ to cytidine solution led to

dx.doi.org/10.1021/la5028702 | Langmuir 2014, 30, 10910−10917

almost no change of the relevant peak absorption, as shown in Figure S3 of the Supporting Information. In comparison, it is observed that although both A-Au (Figure 2A-c; Figure 2C, red trace) and A-AuAg (Figure 2B-c′; Figure 2D, red trace) solutions have strong fluorescence equivalent to that of C-AuAg NCs, but they are unstable, and after being stored in the same condition for just 1 h, the relevant solution emerges obvious green precipitate and the clear supernatant have only weak fluorescence (Figure S1B, Supporting Information). When the adding sequence of $HAuCl_4$ and $AgNO_3$ is reversed, there is no fluorescence (Figure 2A-b,d) or only very weak fluorescence to be found (Figure 2B-b′,d′). These observations could be attributed to the various structures of cytidine and adenosine (Figure S4, Supporting Information), at pH 6.5, and the N7 position might be involved in binding to gold for adenosine, while for cytidine both the N3 nitrogen and the keto oxygen might bind to gold.[26] The binding sites and binding affinities are both different so as to influence the diameter and dispersity of C-AuAg NCs and A-AuAg products. Base carbonyl oxygens and doubly bonded ring nitrogens of cytidine and adenosine are often used for binding to metal ions, but the exocyclic amino groups are poor ligands since their lone-pair electron is delocalized.[3,25] Moreover, time-dependent density functional theory has suggested that Ag NCs prefer to bind to the doubly bonded ring nitrogens.[3,37] Some literature reported that adenosine-mediated Au solution emerges aggregation due to a lack of charge,[8] thus, even if the addition of $AgNO_3$ to adenosine/Au solution, it could not prevent the generation of the precipitate. In Schultz's paper,[28,29] work on DNA and RNA homopolymer strands of the canonical bases and reducing with $NaBH_4$ found fluorescent products for G and C, but not A, T, or U. In this work, we found that cytidine and adenosine produced fluorescent Au NCs and AuAg NCs reducing with citrate, but there is no fluorescent products emerging after cytidine or adenosine mixed with $AgNO_3$ under the same conditions. It is evident that the formation of fluorescent products is influenced by many factors, such as the existence form of the bases (e.g., monomeric or DNA and RNA homopolymer strands) and the difference of reductant (e.g., citrate, $NaBH_4$, or others) as well as the relevant metal ions (e.g., gold ions or silver ions and others). All these factors influence the formation of fluorescent products. For example, Liu and co-workers[26] have prepared blue-emitting gold nanoclusters in the presence of polycytosine DNAs at low pH and polyadenine at neutral pH using citrate as the reducing agent. Under our experimental conditions, only cytidine and adenosine produced fluorescent nanocluster products.

Based on the above observations, the factors influencing the formation of fluorescent C-AuAg NCs have been further explored. As shown in Figure 3A,B, the heating time is identified to be the key factor to produce relevant fluorescence intensity. At 80 °C, the fluorescence reached the maximum for about 1 h. Further heating led to fluorescence intensity decrease. Besides, the molar ratios of cytidine to $HAuCl_4$ and $HAuCl_4$ to $AgNO_3$ also influence the fluorescence intensity or emission peak position of C-AuAg NCs (Figure 3C−F). The reduction agent citrate is also essential since no fluorescence could be produced without it (Figure S5, Supporting Information), indicating that citrate may act as an effective stabilizer that prevents agglomeration of the clusters. It is noteworthy that the absence of cytidine will render the quick reduction of $HAuCl_4$ and $AgNO_3$ by citrate to generate black nonfluorescent precipitate. On the basis of relevant studies, the

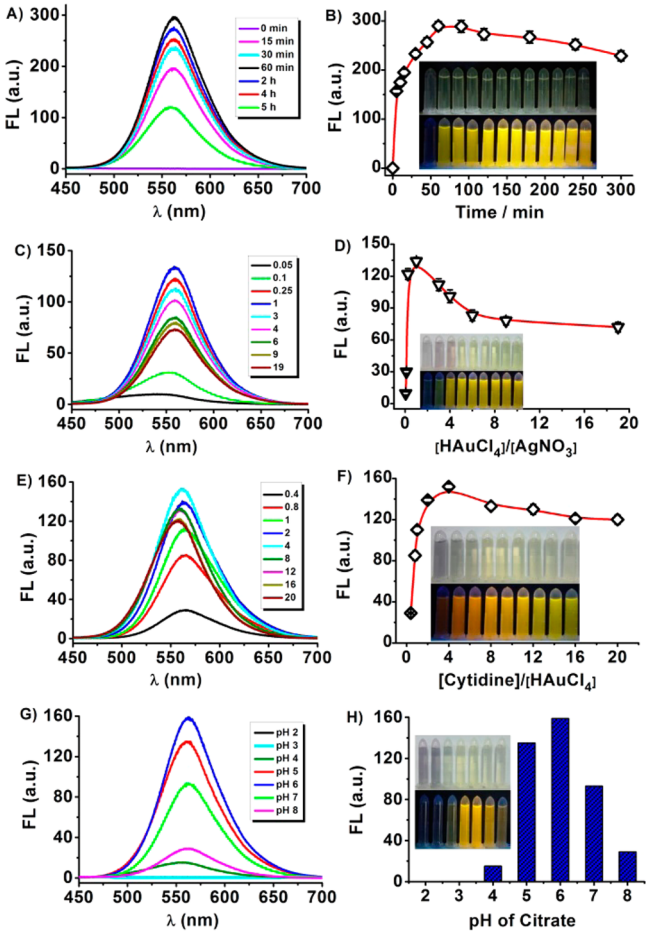

Figure 3. Emission spectra and fluorescence evolution of C-AuAg NCs with different heating time at 80 °C water bath (A, B), different $HAuCl_4$ and $AgNO_3$ molar ratio (C, D), different concentration of cytidine (E, F), different pH citrate buffer (G, H). Inset: optical and fluorescence (excited at 365 nm) photographs of C-AuAg NCs. From left to right, (B inset) the heating time is 0, 5, 10, 15, 30, 45, 60, 75, 90, 120, 180, 240, and 300 min. Other conditions: [cytidine] = 4 mM, $[HAuCl_4] = [AgNO_3] = 0.25$ mM; (D inset) $[HAuCl_4]/[AgNO_3]$ = 0.05, 0.1, 0.25, 1, 3, 4, 6, 9, and 19. Other conditions: [cytidine] = 4 mM; (F inset) $[cytidine]/[HAuCl_4]$ = 0.4, 0.8, 1, 2, 4, 8, 12, 18, and 20. Other conditions: $[HAuCl_4] = [AgNO_3] = 0.25$ mM; (H inset) The pH of the citrate is 2, 3, 4, 5, 6, 7, and 8. Other conditions: [cytidine] = 1 mM, $[HAuCl_4] = [AgNO_3] = 0.25$ mM. For all samples the concentration of citrate is 50 mM.

following research was performed by choosing optimal conditions at 80 °C for 1 h with the molar ratio of cytidine:$HAuCl_4$:$AgNO_3$ = 4:1:1.

The pH values of citrate buffer also play important role in the synthesis of C-AuAg NCs (Figure 3G,H). When the pH value of citrate buffer is 6, the relevant fluorescence reached maximum. Because of the protonation effect of cytidine (pK_a = 4.2),[3,33] protonation of cytidine at pH 2 and 3 inhibited the related synthesis, and therefore the N3[33,38,39] position might be involved in binding to gold.

Therefore, to understand the performance of Ag^+ enhancing the fluorescence of C-Au NCs, several possibilities were considered: (1) silver ions form some fluorescent C-Ag complexes; (2) silver ions themselves form fluorescent species when reduced by citrate or C-Au NCs; (3) oxidation of C-Au NCs results in enhancement of its own fluorescence; (4) silver ions interact with C-Au NCs and cause the fluorescence

dx.doi.org/10.1021/la5028702 | Langmuir 2014, 30, 10910−10917

enhancement (with the composition of C-Au NCs unchanged); and (5) the reduced silver species interact with C-Au NCs and lead to the fluorescence enhancement. Below we will consider and verify all the above possibilities one by one.

The fact that the mixture of cytidine, $AgNO_3$, and citrate shows negligible luminescence excludes the first and second possibilities. Oxidation of C-Au NCs by H_2O_2 does lead to significant enhancement, thus proving that the third possibility is possible (Figure S6, Supporting Information). To determine whether the Ag^+ has been reduced to Ag^0 or not, XPS analysis was conducted to determine the content and oxidation states of the metals in samples. As shown in Figure S7A of the Supporting Information, gold and silver were found in the XPS. Figure 5A shows the Au 4f spectrum resolved into spin−orbit components. The Au $4f_{7/2}$ and $4f_{5/2}$ peaks occur at a binding energy (BE) of 83.8 and 87.5 eV, respectively, indicating the formation of Au(0).[23,40] The Ag 3d spectrum (Figure 5B) also resolved into two spin−orbit components. As shown in Figure 4D, the sample results in two energy peaks at 367.4 and 373.4

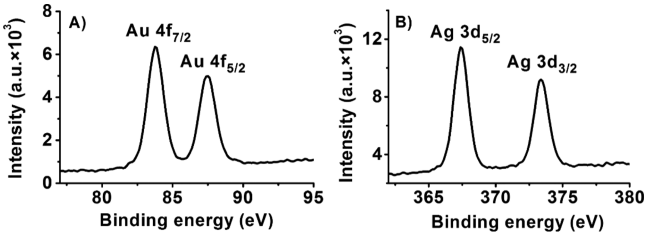

Figure 4. XPS survey spectra of Au 4f (A) and Ag 3d (B) in the C-AuAg NCs.

eV, which is consistent with the result obtained for Ag NCs;[23] they are assigned for the Ag $3d_{5/2}$ and Ag $3d_{3/2}$, respectively. Note that there is not much difference in BE between Ag(0) and Ag(I) states due to the close proximity of their binding energies.[13,36] Moreover, adding excess EDTA to the C-AuAg NCs solution, we found that there is no change for the fluorescence intensity of C-AuAg NCs, indicating the absence of free Ag^+ in C-Au NCs. Maybe Ag^+ has a strong interaction with C-Au NCs so that EDTA and Ag^+ do not produce complexation (Figure S8, Supporting Information). By combining with the XPS analysis, the fourth and fifth possibility of silver ions or reduced silver species interacting with C-Au NCs and causing the fluorescence enhancement are possible. The results are consistent with that of the literature reported.[10] That is the chelation-enhanced fluorescence (CHEF) mechanism, and silver ions can readily interact with C-Au nanoclusters and lead to the fluorescence enhancement.[10,41] As metal-enhanced fluorescence (MEF) effect, reduced silver species interacting with C-Au nanoclusters can produce fluorescence enhancement.[10,42] Last but not least, the oxidation state of relevant clusters is likely to result in the enhancement of its own fluorescence.[10] Notably the binding of cytidine to AuAg NCs is demonstrated by the presence of N 1s at binding energies of 398.6 eV (Figure S7B, Supporting Information).[40,43]

The size of C-AuAg NCs is evaluated by TEM. A size analysis indicated the presence of 1.50 ± 0.31 nm particles of relatively narrow size distribution and higher magnification of the particles (Figure 5A,B) shows the crystallinity of the particles with no change in size and obvious alteration due to the presence of silver compared with C-Au nanoclusters

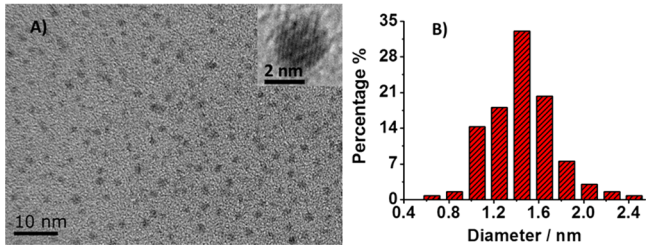

Figure 5. Typical TEM image of C-AuAg NCs (A). Inset: high-resolution image with the crystallinity of the metallic structure. (B) Size distribution histogram of C-AuAg NCs by counting 134 particles.

(Figure S9B, Supporting Information). The imaged particles in TEM looked larger than the actual fluorescent product, which might be related to the high-energy e-beam-induced melting of the metal core to some extent.[23] EDS study of C-AuAg NCs shows the expected elements (Figure S9A, Supporting Information), but the elements ratio of silver to gold is different from that detected by XPS. Considering that XPS and EDS both are semiquantitative spectrographic analysis methods, the XPS detection is mainly focused on the location of the sample surfaces while for EDS it could detect 1 μm depth of the samples. XPS detection can reach a much larger region compared to EDS detection; thus, the different results are possible. Meanwhile, in order to determine the Au and Ag content, the relevant samples have been also measured by inductively coupled plasma mass spectrometry (ICP-MS). The results of ICP-MS analysis indicate that the molar ratio of Au:Ag in the fluorescent C-AuAg NCs is 19.5:1.

FT-IR study of C-AuAg NCs shows the presence of citrate. The characteristic bands, i.e., at around 1394 and 1591 cm^{-1} for the symmetric stretching and the antisymmetric stretching of COO^-, respectively, are clearly seen in the FT-IR spectrum of the pure trisodium citrate (Figure 6B, red line).[44] However,

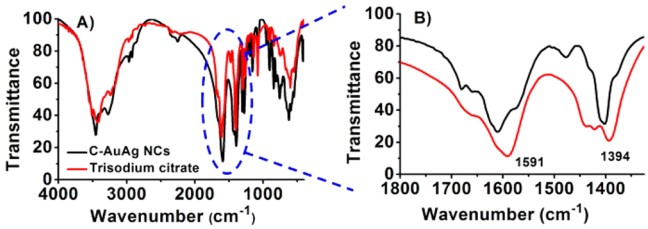

Figure 6. (A) FT-IR spectra of pure trisodium citrate, C-AuAg NCs. (B) Enlargement of the region surrounded by dotted line in (A) from 1320 to 1800 cm^{-1}.

these characteristic bands have a red-shift to 1402 and 1610 cm^{-1} in the FT-IR spectrum of C-AuAg NCs (Figure 6B, black line). Trisodium citrate features in the region of 4000−500 cm^{-1} confirm C-AuAg NCs was protected by trisodium citrate. Trisodium citrate is a reduction agent, and without it there are no fluorescent NCs which could be produced (Figure S5, Supporting Information). It is noteworthy that the absence of cytidine will render the quick reduction of $HAuCl_4$ and $AgNO_3$ by citrate to generate black nonfluorescent precipitate. In this work, cytidine acts as a stabilizer to form nanoclusters while the reduction of metal ions is through citrate. Because of the low concentration of cytidine (1 mM) compared with citrate (50 mM), its FT-IR spectrum may be masked by the latter.

Photographs of C-AuAg NCs and the relevant solid synthesized product are shown in Figure 7. A little yellowish-

dx.doi.org/10.1021/la5028702 | Langmuir 2014, 30, 10910−10917

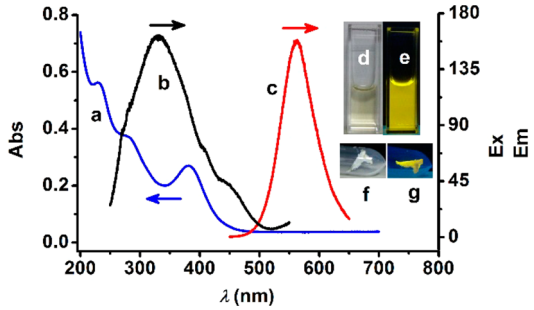

Figure 7. Optical characterization of the C-AuAg NCs. Curves a, b, and c show the UV/vis absorption spectrum, the excitation spectrum (Ex), and the emission spectrum (Em) of the C-AuAg NCs, respectively. Inset: photographs of nanoclusters in water (d, e) and in the solid state (f, g) under visible (d, f) and UV light (excited at 365 nm; e, g).

white precipitate was removed upon filtering and centrifugation to get a transparent primrose yellow supernatant. Then, the supernatant was purified and collected for vacuum-drying, and a solid sample was obtained for analysis (for details see the Experimental Section). The materials, in both solution and solid states, show bright emission that can be photographed (inset in Figure 7). Furthermore, the UV/vis absorption and fluorescence spectrum of C-AuAg NCs demonstrate that the absorption peaks emerged at 230, 280, and 380 nm (Figure 7, curve a). The excitation spectrum of C-AuAg NCs (i.e., excitation peak at ca. 330 nm) is obviously different from the absorption spectrum (Figure 7, curve a). Maybe for nanoclusters, the particle size is small to approach the Fermi wavelength of an electron (ca. 0.5 nm for silver and gold), and the continuous density of states breaks up into discrete energy levels. Therefore, optical and electronic properties of nanoclusters are significantly different to relevant big nanoparticles.[45−47] Moreover, the as-synthesized clusters are stable for months in aqueous phase by storing at low temperatures (Figure S10, Supporting Information) and in solid state at room temperature.

The fluorescence quantum yields and chemical yields were measured. The chemical yield obtained is ca. 57.8%. The fluorescence quantum yield is measured to be around 9% by using the comparative method with Rhodamine B (QY = 95% in ethanol) (see the Supporting Information). This result confirms the high brightness of the clusters in water and the significant fluorescence enhancement compared to most of the fluorescent gold clusters reported in the literature.[13] Several noble metal clusters have shown remarkably long fluorescence lifetimes of 1 or 2 orders of magnitude higher than organic dyes and quantum dots.[13,48] C-AuAg NCs exhibit a fluorescence lifetime with a biexponential decay: a long component τ_1 (12.9 ± 0.17 μs) and a short component τ_2 (3.2 ± 0.09 μs) with percentage 29.8% and 70.2%, respectively (Figure S11, Supporting Information). Dickson et al. attributed the long lifetime component to the electron transfer from the clusters to the ligand where a redox process might occur.[49] They further suggested that the decay on the microsecond time scale was the result of a charge-separated trap.

Consequently, a new strategy of rapid synthesis of highly fluorescent AuAg NCs in the mediate of cytidine has been developed. Considering the possible overexpress of modified nucleoside and other relevant biomolecules in cancer human body fluids, we take human serum as an example to explore the potential of the relevant promising application for highly sensitive and rapid biomedical survey. The fresh human serum samples (i.e., leukemia human serum and normal human serum samples) were obtained from the local hospital and used as testing samples. The experiment protocol is same as the synthesis of C-AuAg NCs, only use of proper serum samples to substitute the commercial reagent of cytidine (for details see the Experimental Section). After 1 h incubation in 37 °C water bath, the fluorescence of all samples was measured. As shown in Figure S12, based on the fluorescence study of *in situ* biosynthesis of AuAg NCs, there is obvious difference at the fluorescence emission spectra between cancerous and normal human serums excited at the same wavelength (330 nm), demonstrating the potential application of the strategy for the possible recognition and analysis of some disease related changes in blood serum or other physiological real clinical samples.

CONCLUSION

In summary, a novel type of strategy taking cytidine as template to rapid synthesis of highly fluorescent AuAg NCs has been developed. The TEM, XPS, fluorescence, and FT-IR characterization validate that C-AuAg NCs with a diameter of 1.50 ± 0.31 nm, a quantum yield ∼9%, and an average lifetime ∼6.07 μs possess prominent fluorescence properties, good dispersibility, and easy water solubility. The availability of both fluorescent nanoclusters and molecular species allows us to employ a diverse range of techniques to gain a more complete understanding of the relevant bioprocess. Furthermore, this strategy by rapid producing of highly fluorescent nanoclusters could be further explored for the possible recognition of some disease related changes in blood serum, indicating the potential and promising application in relevant bioanalysis and biomedical diagnosis.

ASSOCIATED CONTENT

Supporting Information

Additional fluorescent spectra and characterization data of nanoclusters (UV/vis spectra, full-range XPS spectra, lifetime decay profile, quantum yield). This material is available free of charge via the Internet at http://pubs.acs.org.

AUTHOR INFORMATION

Corresponding Author

*E-mail xuewang@seu.edu.cn; Tel +86-25-83792177 (X.W.).

Notes

The authors declare no competing financial interest.

ACKNOWLEDGMENTS

This work is supported by the National Basic Research Program (2010CB732404) and National Natural Science Foundation of China (81325011, 21327902), National High Technology Research and Development Program of China (2012AA022703), and Suzhou Science & Technology Major Project (ZXY2012028).

REFERENCES

(1) Shang, L.; Dong, S.; Nienhaus, G. U. Ultra-Small Fluorescent Metal Nanoclusters: Synthesis and Biological Applications. *Nano Today* **2011**, *6*, 401−418.

(2) Zhang, L. B.; Wang, E. K. Metal Nanoclusters: New Fluorescent Probes for Sensors and Bioimaging. *Nano Today* **2014**, *9*, 132−157.

(3) Shiang, Y.-C.; Huang, C.-C.; Chen, W.-Y.; Chen, P.-C.; Chang, H.-T. Fluorescent Gold and Silver Nanoclusters for the Analysis of Biopolymers and Cell Imaging. *J. Mater. Chem.* **2012**, *22*, 12972−12982.
(4) Xu, H.; Suslick, K. S. Water-Soluble Fluorescent Silver Nanoclusters. *Adv. Mater.* **2010**, *22*, 1078−1082.
(5) Ma, K.; Shao, Y.; Cui, Q.; Wu, F.; Xu, S.; Liu, G. Base-Stacking-Determined Fluorescence Emission of DNA Abasic Site-Templated Silver Nanoclusters. *Langmuir* **2012**, *28*, 15313−15322.
(6) Wen, F.; Dong, Y.; Feng, L.; Wang, S.; Zhang, S.; Zhang, X. Horseradish Peroxidase Functionalized Fluorescent Gold Nanoclusters for Hydrogen Peroxide Sensing. *Anal. Chem.* **2011**, *83*, 1193−1196.
(7) Fernandez-Iglesias, N.; Bettmer, J. Synthesis, Purification and Mass Spectrometric Characterisation of A Fluorescent Au-9@BSA Nanocluster and Its Enzymatic Digestion by Trypsin. *Nanoscale* **2014**, *6*, 716−721.
(8) Draz, M. S.; Fang, B. A.; Li, L.; Chen, Z.; Wang, Y.; Xu, Y.; Yang, J.; Killeen, K.; Chen, F. F. Hybrid Nanocluster Plasmonic Resonator for Immunological Detection of Hepatitis B Virus. *ACS Nano* **2012**, *6*, 7634−7643.
(9) Bootharaju, M. S.; Pradeep, T. Investigation into the Reactivity of Unsupported and Supported Ag_7 and Ag_8 Clusters with Toxic Metal Ions. *Langmuir* **2011**, *27*, 8134−8143.
(10) Wu, Z.; Wang, M.; Yang, J.; Zheng, X.; Cai, W.; Meng, G.; Qian, H.; Wang, H.; Jin, R. Well-Defined Nanoclusters as Fluorescent Nanosensors: A Case Study on $Au_{25}(SG)_{18}$. *Small* **2012**, *8*, 2028−2035.
(11) Dai, H.; Shi, Y.; Wang, Y.; Sun, Y.; Hu, J.; Ni, P.; Li, Z. Label-Free Turn-On Fluorescent Detection of Melamine Based on the Anti-Quenching Ability of Hg^{2+} to Gold Nanoclusters. *Biosens. Bioelectron.* **2014**, *53*, 76−81.
(12) Wang, J.; Zhang, G.; Li, Q.; Jiang, H.; Liu, C.; Amatore, C.; Wang, X. *In vivo* Self-bio-Imaging of Tumors Through *in situ* Biosynthesized Fluorescent Gold Nanoclusters. *Sci. Rep.* **2013**, *3*, 1157−1162.
(13) Le Guevel, X.; Trouillet, V.; Spies, C.; Li, K.; Laaksonen, T.; Auerbach, D.; Jung, G.; Schneider, M. High Photostability and Enhanced Fluorescence of Gold Nanoclusters by Silver Doping. *Nanoscale* **2012**, *4*, 7624−7631.
(14) Esumi, K.; Isono, R.; Yoshimura, T. Preparation of PAMAM-and PPI-Metal (Silver, Platinum, and Palladium) Nanocomposites and Their Catalytic Activities for Reduction of 4-Nitrophenol. *Langmuir* **2004**, *20*, 237−243.
(15) Tao, Y.; Lin, Y.; Huang, Z.; Ren, J.; Qu, X. Incorporating Graphene Oxide and Gold Nanoclusters: A Synergistic Catalyst with Surprisingly High Peroxidase-Like Activity Over A Broad pH Range and Its Application for Cancer Cell Detection. *Adv. Mater.* **2013**, *25*, 2594−2599.
(16) Kon, K.; Siddiki, S.; Shimizu, K. I. Size-and Support-Dependent Pt Nanocluster Catalysis for Oxidant-Free Dehydrogenation of Alcohols. *J. Catal.* **2013**, *304*, 63−71.
(17) Jin, R. Quantum Sized, Thiolate-Protected Gold Nanoclusters. *Nanoscale* **2010**, *2*, 343−362.
(18) Wu, Z.; Jin, R. On the Ligand's Role in the Fluorescence of Gold Nanoclusters. *Nano Lett.* **2010**, *10*, 2568−2573.
(19) Ganguly, M.; Pal, A.; Negishi, Y.; Pal, T. Synthesis of Highly Fluorescent Silver Clusters on Gold (I) Surface. *Langmuir* **2013**, *29*, 2033−2043.
(20) Zheng, J.; Dickson, R. M. Individual Water-Soluble Dendrimer-Encapsulated Silver Nanodot Fluorescence. *J. Am. Chem. Soc.* **2002**, *124*, 13982−13983.
(21) Liu, S.; Lu, F.; Zhu, J. J. Highly Fluorescent Ag Nanoclusters: Microwave-Assisted Green Synthesis and Cr^{3+} Sensing. *Chem. Commun.* **2011**, *47*, 2661−2663.
(22) Xie, J.; Zheng, Y.; Ying, J. Y. Protein-Directed Synthesis of Highly Fluorescent Gold Nanoclusters. *J. Am. Chem. Soc.* **2009**, *131*, 888−889.
(23) Li, H.-W.; Yue, Y.; Liu, T.-Y.; Li, D.; Wu, Y. Fluorescence-Enhanced Sensing Mechanism of BSA-Protected Small Gold-Nanoclusters to Silver(I) Ions in Aqueous Solutions. *J. Phys. Chem. C* **2013**, *117*, 16159−16165.
(24) Yang, X.; Gan, L.; Han, L.; Wang, E.; Wang, J. High-Yield Synthesis of Silver Nanoclusters Protected by DNA Monomers and DFT Prediction of their Photoluminescence Properties. *Angew. Chem., Int. Ed.* **2013**, *125*, 2076−2080.
(25) Liu, J. Adsorption of DNA onto Gold Nanoparticles and Graphene Oxide: Surface Science and Applications. *Phys. Chem. Chem. Phys.* **2012**, *14*, 10485−10496.
(26) Kennedy, T. A.; MacLean, J. L.; Liu, J. Blue Emitting Gold Nanoclusters Templated by Poly-Cytosine DNA at Low pH and Poly-Adenine DNA at Neutral pH. *Chem. Commun.* **2012**, *48*, 6845−6847.
(27) Schultz, D.; Gardner, K.; Oemrawsingh, S. S.; Markešević, N.; Olsson, K.; Debord, M.; Bouwmeester, D.; Gwinn, E. Evidence for Rod-Shaped DNA-Stabilized Silver Nanocluster Emitters. *Adv. Mater.* **2013**, *25*, 2797−2803.
(28) Schultz, D.; Gwinn, E. G. Silver Atom and Strand Numbers in Fluorescent and Dark Ag: DNAs. *Chem. Commun.* **2012**, *48*, 5748−5750.
(29) Schultz, D.; Gwinn, E. Stabilization of Fluorescent Silver Clusters by RNA Homopolymers and Their DNA Analogs: C, G versus A, T(U) Dichotomy. *Chem. Commun.* **2011**, *47*, 4715−4717.
(30) Sengupta, B.; Springer, K.; Buckman, J. G.; Story, S. P.; Abe, O. H.; Hasan, Z. W.; Prudowsky, Z. D.; Rudisill, S. E.; Degtyareva, N. N.; Petty, J. T. DNA Templates for Fluorescent Silver Clusters and I-Motif Folding. *J. Phys. Chem. C* **2009**, *113*, 19518−19524.
(31) Sharma, J.; Yeh, H. C.; Yoo, H.; Werner, J. H.; Martinez, J. S. A Complementary Palette of Fluorescent Silver Nanoclusters. *Chem. Commun.* **2010**, *46*, 3280−3282.
(32) Sengupta, B.; Ritchie, C. M.; Buckman, J. G.; Johnsen, K. R.; Goodwin, P. M.; Petty, J. T. Base-Directed Formation of Fluorescent Silver Clusters. *J. Phys. Chem. C* **2008**, *112*, 18776−18782.
(33) Lopez, A.; Liu, J. Light-Activated Metal-Coordinated Supramolecular Complexes with Charge-Directed Self-Assembly. *J. Phys. Chem. C* **2013**, *117*, 3653−3661.
(34) Speer, J.; Gehrke, C. W.; Kuo, K. C.; Waalkes, T. P.; Borek, E. tRNA Breakdown Products as Markers for Cancer. *Cancer* **1979**, *44*, 2120−2123.
(35) Zheng, Y. F.; Kong, H. W.; Xiong, J. H.; Lv, S.; Xu, G. W. Clinical Significance and Prognostic Value of Urinary Nucleosides in Breast Cancer Patients. *Clin. Biochem.* **2005**, *38*, 24−30.
(36) Udayabhaskararao, T.; Sun, Y.; Goswami, N.; Pal, S. K.; Balasubramanian, K.; Pradeep, T. Ag_7Au_6: A 13-Atom Alloy Quantum Cluster. *Angew. Chem., Int. Ed.* **2012**, *51*, 2155−2159.
(37) Soto-Verdugo, V.; Metiu, H.; Gwinn, E. The Properties of Small Ag Clusters Bound to DNA Bases. *J. Chem. Phys.* **2010**, *132*, 195102−195112.
(38) Sánchez-Cortés, S.; Molina, M.; García-Ramos, J.; Carmona, P. Interactions of Cytidine Derivatives with Metals as Revealed by Surface-Enhanced Raman Spectroscopy. *J. Raman Spectrosc.* **1991**, *22*, 819−824.
(39) Holowczak, M. S.; Stancl, M. D.; Wong, G. B. Trichloro(1-methylcytosinato)gold(III). Model for Gold-DNA Interactions. *J. Am. Chem. Soc.* **1985**, *107*, 5789−5790.
(40) Zhao, W.; Gonzaga, F.; Li, Y.; Brook, M. A. Highly Stabilized Nucleotide-Capped Small Gold Nanoparticles with Tunable Size. *Adv. Mater.* **2007**, *19*, 1766−1771.
(41) Al-Kady, A. S.; Gaber, M.; Hussein, M. M.; Ebeid, E.-Z. M. Fluorescence Enhancement of Coumarin Thiourea Derivatives by Hg^{2+}, Ag^{+}, and Silver Nanoparticles. *J. Phys. Chem. A* **2009**, *113*, 9474−9484.
(42) Pan, S.; Wang, Z.; Rothberg, L. J. Enhancement of Adsorbed Dye Monolayer Fluorescence by A Silver Nanoparticle Overlayer. *J. Phys. Chem. B* **2006**, *110*, 17383−17387.
(43) Petrovykh, D. Y.; Kimura-Suda, H.; Whitman, L. J.; Tarlov, M. J. Quantitative Analysis and Characterization of DNA Immobilized on Gold. *J. Am. Chem. Soc.* **2003**, *125*, 5219−5226.
(44) Zou, X.; Ying, E.; Dong, S. Seed-Mediated Synthesis of Branched Gold Nanoparticle with the Assistance of Citrate and Their

Surface-Enhanced Raman Scattering Properties. *Nanotechnology* **2006**, *17*, 4758−4764.
(45) Vosch, T.; Antoku, Y.; Hsiang, J. C.; Richards, C. I.; Gonzalez, J. I.; Dickson, R. M. Strongly Emissive Individual DNA-Encapsulated Ag Nanoclusters as Single-Molecule Fluorophores. *Proc. Natl. Acad. Sci. U. S. A.* **2007**, *104*, 12616−12621.
(46) Shen, Z.; Duan, H.; Frey, H. Water-Soluble Fluorescent Ag Nanoclusters Obtained from Multiarm Star Poly(acrylic acid) as "Molecular Hydrogel" Templates. *Adv. Mater.* **2007**, *19*, 349−352.
(47) Zheng, J.; Zhou, C.; Yu, M.; Liu, J. Different Sized Luminescent Gold Nanoparticles. *Nanoscale* **2012**, *4*, 4073−4083.
(48) Le Guével, X.; Hötzer, B.; Jung, G.; Hollemeyer, K.; Trouillet, V.; Schneider, M. Formation of Fluorescent Metal (Au, Ag) Nanoclusters Capped in Bovine Serum Albumin Followed by Fluorescence and Spectroscopy. *J. Phys. Chem. C* **2011**, *115*, 10955−10963.
(49) Patel, S. A.; Cozzuol, M.; Hales, J. M.; Richards, C. I.; Sartin, M.; Hsiang, J.-C.; Vosch, T.; Perry, J. W.; Dickson, R. M. Electron Transfer-Induced Blinking in Ag Nanodot Fluorescence. *J. Phys. Chem. C* **2009**, *113*, 20264−20270.